Optical control of backward and forward microwave generation

Sankar Davuluri and Yuri Rostovtsev*
Department of Physics, University of North Texas, 1155 Union Circle, No. 311427, Denton, Texas 76203, USA
(Received 21 January 2013; revised manuscript received 16 July 2013; published 27 November 2013)

We propose an experiment to demonstrate a strong coherent backward and forward microwave generation using forward-propagating optical fields only. This is achieved by applying laser fields to an ultradispersive medium with properly chosen detunings and/or Rabi frequencies to excite a spin coherence that generates a forward- or backward-propagating microwave. Applications to coherent scattering and remote sensing are discussed.

DOI: 10.1103/PhysRevA.88.053847 PACS number(s): 42.50.Gy, 42.65.Ky, 78.47.jh

I. INTRODUCTION

Alkali-metal atoms [1] provide perfect opportunities for simultaneous coupling with optical and microwave fields. The optical fields can create quantum coherence at the hyperfine transitions and a microwave field can couple the transitions between the hyperfine structures (see Fig. 1).

Quantum coherence [2–4] has been shown to result in many counterintuitive phenomena. Scattering via a gradient force in gases [5], forward Brillouin scattering in ultradispersive resonant media [6,7], electromagnetically induced transparency [8–14], Fano and enhanced Kerr effects [12,15], slow light [16–19], enhancement of the Fizeau effect [20], Doppler broadening elimination [21], buffer-gas-induced narrow absorption resonances [22], light-induced chirality in nonchiral medium [23], a new class of entanglement amplifier [24] based on correlated spontaneous emission lasers [25,26], lasing without population inversion [27] and also without hidden inversion in the reservoir [28], coherent-enhanced lasing [29], improvement of the efficiency of thermal engines [30] and solar cells [31], and coherent Raman scattering enhancement via maximal coherence in atoms [32] and biomolecules [33–35] are a few examples that demonstrate the importance of quantum coherence. The possibility of control of four-wave mixing has been discussed [36], and plasma-assisted coherent backscattering for standoff spectroscopy was proposed in [37].

The phenomenon of coherent microwave-stimulated emission [38–41] in a cavity was analyzed for the case of alkali-metal atoms such as Cs and Rb under coherent population trapping in a Λ scheme. Microwave emission has been observed at the ground-state hyperfine transition frequency of a cesium atomic vapor driven into a nonabsorbing state by means of coherent population trapping. The coherent emission observed is due to the oscillating magnetic dipoles generated by the coherence which is induced between the ground-state hyperfine levels when they are coupled to an excited state by means of two laser radiations as shown in Fig. 1. In this paper, we analyze the possibilities of optical control of nonlinear microwave generation.

II. MODEL

The geometry and configuration of the fields are shown in Fig. 1. The Rb levels have the fine structure resulting from the L-S coupling, where L is the orbital motion of the atomic electron and $S=1/2$ is the spin of the electron. The fine structure is determined by the total electron angular moment $J=L+S$. The states are

$$|J,m_J\rangle = \sum C^{Jm_J}_{Lm_L,Im_I}|Lm_L,Sm_S\rangle, \tag{1}$$

where $C^{Jm_J}_{Lm_L,Im_I}$ are the Clebsch-Gordon coefficients. The hyperfine structure occurs due to the spin of the nucleus ($I=3/2$), which should be added to form the total angular momentum $F=J+I$:

$$|F,m_F\rangle = \sum C^{Fm_F}_{Jm_J,Im_I}|Jm_J,Im_I\rangle, \tag{2}$$

where $C^{Fm_F}_{Jm_j;Im_I}$ are the corresponding Clebsch-Gordon coefficients.

At this point, we assume that all populations have been prepared in the state $|F=1,1\rangle$ using optical pumping [42]. More details about a particular pumping scheme are provided below. Let us consider the levels shown in Fig. 1. To form a three-level system, the upper levels can be

$$\begin{aligned}|a\rangle &= |F'=1,m\rangle\\ &= \frac{1}{2}[-\sqrt{2-m}|P_{1/2},m=1/2\rangle|I=3/2,m-1/2\rangle\\ &\quad+\sqrt{2+m}|P_{1/2},m=-1/2\rangle|I=3/2,m+1/2\rangle],\\ |a\rangle &= |F'=2,m\rangle\\ &= \frac{1}{2}[\sqrt{2+m}|P_{1/2},m=1/2\rangle|I=3/2,m-1/2\rangle\\ &\quad+\sqrt{2-m}|P_{1/2},m=-1/2\rangle|I=3/2,m+1/2\rangle],\end{aligned}$$

where

$$\begin{aligned}|P_{1/2},m\rangle = \frac{1}{\sqrt{3}}[&-\sqrt{3/2-m}|P,m-1/2\rangle|m_s=1/2\rangle\\ &+\sqrt{3/2+m}|P,m+1/2\rangle|m_s=-1/2\rangle].\end{aligned}$$

In particular, for level $|a\rangle$ we can choose

$$\begin{aligned}|a\rangle &= |F'=1,1\rangle\\ &= \frac{1}{2}[-|P_{1/2},m=1/2\rangle|I=3/2,1/2\rangle\\ &\quad+\sqrt{3}|P_{1/2},m=-1/2\rangle|I=3/2,3/2\rangle]\end{aligned} \tag{3}$$

or

$$\begin{aligned}|a\rangle = |F'=2,1\rangle = \frac{1}{2}[&\sqrt{3}|P_{1/2},m=1/2\rangle|I=3/2,1/2\rangle\\ &+|P_{1/2},m=-1/2\rangle|I=3/2,3/2\rangle],\end{aligned}$$

*rost@unt.edu

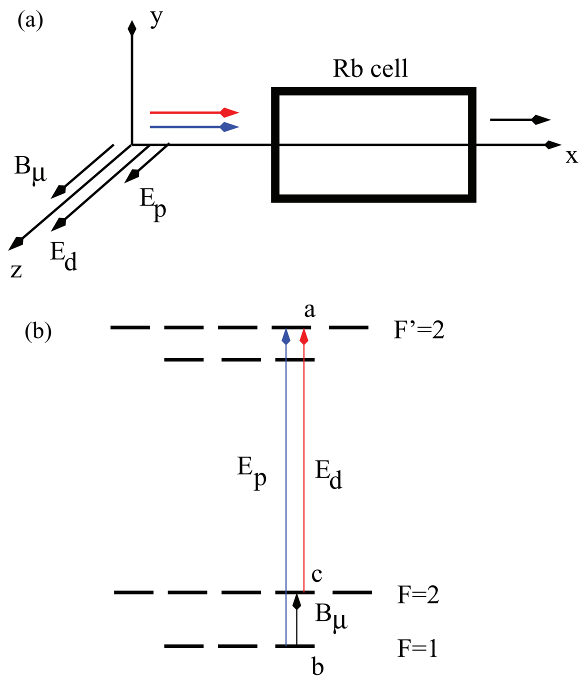

FIG. 1. (Color online) (a) Configuration of the electric fields of optical beams and magnetic field of microwave radiation. (b) Atomic Rb level scheme for implementation of coherent backscattering.

and for the ground states, we choose

$$|b\rangle = |F=1,m=1\rangle = \frac{|S\rangle}{2}[-|I,1/2\rangle|m_s=1/2\rangle + \sqrt{3}|I,3/2\rangle|m_s=-1/2\rangle], \tag{4}$$

$$|c\rangle = |F=2,m=1\rangle = \frac{|S\rangle}{2}[\sqrt{3}|I,1/2\rangle|m_s=1/2\rangle + |I,3/2\rangle|m_s=-1/2\rangle]. \tag{5}$$

The interaction Hamiltonian of the system can be written as

$$V_I = -\hbar[\tilde{\Omega}_1 e^{-i\omega_{ab}t}|a\rangle\langle b| + \tilde{\Omega}_2 e^{-i\omega_{ac}t}|a\rangle\langle c| + \text{H.c.}] \tag{6}$$

$$-\hbar[\tilde{\Omega}_3 e^{-i\omega_{cb}t}|c\rangle\langle b| + \text{H.c.}], \tag{7}$$

where ω_{ab}, ω_{ac}, and ω_{cb} are the frequency differences between the corresponding atomic energy levels, $\tilde{\Omega}_1 = \wp_{ab}E_p/\hbar$ and $\tilde{\Omega}_2 = \wp_{ac}E_d/\hbar$ are the Rabi frequencies corresponding to the optical fields (see Fig. 1), $\wp_{ab}$ and $\wp_{ac}$ are the electric dipole moments of corresponding transitions, $E_p = E_1\cos(\nu_1 t - k_1 x)$ and $E_d = E_2\cos(\nu_2 t - k_2 x)$ are the electric field that have only z components, ν_1 and ν_2 are the frequencies and k_1 and k_2 are the wave vectors of the optical fields, $\tilde{\Omega}_3 = \wp_{ac}B_\mu/\hbar$ is the Rabi frequency corresponding to the magnetic field of the microwave that has only z components, $\wp_{cb}$ is the magnetic dipole moment, $B_\mu = B_3\cos(\nu_3 t \pm k_3 x)$ is the magnetic field of the microwave, plus and minus correspond to the direction of wave propagation, ν_3 and k_3 are the frequency and the wave number of the microwave field, and all E_1, E_2, and B_3 are the slowly varying amplitudes.

The time-dependent density matrix equations are given by

$$\frac{\partial\tilde{\rho}}{\partial t} = -\frac{i}{\hbar}[V_I,\tilde{\rho}] - \frac{1}{2}(\Gamma\tilde{\rho} + \tilde{\rho}\Gamma), \tag{8}$$

where Γ is the relaxation matrix. We write $\tilde{\rho}_{ab} = \rho_{ab}\exp[ik_1x - i\nu_1 t]$, $\tilde{\rho}_{ca} = \rho_{ca}\exp[-ik_2x + i\nu_2 t]$, and $\tilde{\rho}_{cb} = \rho_{cb}\exp[i(k_1-k_2)x - i(\nu_1-\nu_2)t]$ for the off-diagonal elements and $\tilde{\rho}_{ii} = \rho_{ii}$ for the diagonal elements. Then, by using the rotating-wave approximation, the equations of motion for the off-diagonal density matrix elements are

$$\dot{\rho}_{ab} = -\Gamma_{ab}\rho_{ab} + i\Omega_1(\rho_{aa}-\rho_{bb}) - i\rho_{cb}\Omega_2^* + i\rho_{ac}\Omega_3 e^{i\phi},$$
$$\dot{\rho}_{ca} = -\Gamma_{ca}\rho_{ca} + i\Omega_2(\rho_{cc}-\rho_{aa}) + i\rho_{cb}\Omega_1^* - i\rho_{ba}\Omega_3 e^{i\phi},$$
$$\dot{\rho}_{cb} = -\Gamma_{cb}\rho_{cb} + i\rho_{ca}\Omega_1 - i\rho_{ab}\Omega_2 + i\Omega_3 e^{i\phi}(\rho_{cc}-\rho_{bb}),$$

where $\Gamma_{ab} = \gamma_{ab} + i(\omega_{ab}-\nu_1)$, $\Gamma_{ca} = \gamma_{ca} - i(\omega_{ac}-\nu_2)$, and $\Gamma_{cb} = \gamma_{cb} + i(\omega_{cb}-\nu_1+\nu_2)$; $\gamma_{\alpha\beta}$ are the relaxation rates at the corresponding transitions; and $\phi = \Delta\nu t - \Delta k x$, $\Delta\nu = \nu_1 - \nu_2 - \nu_3$, $\Delta k = k_1 - k_2 - k_3$, $\Omega_1 = \wp_{ab}E_1/2\hbar$, $\Omega_2 = \wp_{ac}E_2/2\hbar$, and $\Omega_3 = \wp_{cb}B_3/2\hbar$ are the Rabi frequencies.

To describe the propagation, a self-consistent system also includes the Maxwell equations for all optical and microwave fields,

$$\frac{\partial^2 E_p}{\partial x^2} - \frac{1}{c^2}\frac{\partial^2 E_p}{\partial t^2} = \frac{1}{\epsilon_0 c^2}\frac{\partial^2 P_{ab}}{\partial t^2},$$
$$\frac{\partial^2 E_d}{\partial x^2} - \frac{1}{c^2}\frac{\partial^2 E_d}{\partial t^2} = \frac{1}{\epsilon_0 c^2}\frac{\partial^2 P_{ac}}{\partial t^2},$$
$$\frac{\partial^2 B_3}{\partial x^2} - \frac{1}{c^2}\frac{\partial^2 B_3}{\partial t^2} = \frac{1}{c^2}\frac{\partial^2 M_{cb}}{\partial t^2},$$

where $P_{ab} = N(\wp_{ab}\tilde{\rho}_{ab} + \text{c.c.})$ and $P_{ac} = N(\wp_{ac}\tilde{\rho}_{ac} + \text{c.c.})$ are the optical polarizations, $M_{cb} = N(\wp_{cb}\tilde{\rho}_{cb} + \text{c.c.})$ is the magnetization of the medium, N is the particle density of the medium, and ϵ_0 is the permittivity in vacuum. Using slowly varying amplitude approximation, the propagation equations for the optical and the microwave fields are given by

$$\frac{\partial\Omega_1}{\partial x} + i\left(k_1 - \frac{\nu_1}{c}\right)\Omega_1 = -i\eta_1\rho_{ab}, \tag{9}$$

$$\frac{\partial\Omega_2}{\partial x} + i\left(k_2 - \frac{\nu_2}{c}\right)\Omega_2 = i\eta_2\rho_{ca}, \tag{10}$$

$$\frac{\partial\Omega_3}{\partial x} \pm i\left(k_3 \mp \frac{\nu_3}{c}\right)\Omega_3 = -i\eta_3\rho_{cb}e^{i\Delta kx}, \tag{11}$$

where $\eta_j = \nu_j N|\wp_j|^2/(2\epsilon_0 c\hbar)$ are the coupling constants $(j=1,2,3)$, $\wp_1 = \wp_{ab}$, $\wp_2 = \wp_{ac}$, and $\wp_3 = \wp_{cb}$, and the signs plus and minus correspond to forward and backward propagation of the microwave field. The general relation between changes of the optical fields and the generated microwave field can be established using Eqs. (9)–(11) with the density matrix equations (see Appendix).

The generated microwave field has a Rabi frequency Ω_3 that is much lower than the Rabi frequencies Ω_1 and Ω_2 for optical fields, because the magnetic coupling is much weaker than the optical coupling at the electric dipole transition. Thus, assuming that $|\Omega_3| \ll |\Omega_1|,|\Omega_2|$, we can write the solution of the density matrix equations for the coherences at the optical transitions as

$$\rho_{ab} = i\frac{(\Gamma_{ca}\Gamma_{cb} + |\Omega_1|^2)n_{ab} + |\Omega_2|^2 n_{ca}}{\Gamma_{ab}\Gamma_{ca}\Gamma_{cb} + \Gamma_{ab}|\Omega_1|^2 + \Gamma_{ca}|\Omega_2|^2}\Omega_1, \tag{12}$$

$$\rho_{ca} = i\frac{(\Gamma_{ab}\Gamma_{cb} + |\Omega_2|^2)n_{ca} + |\Omega_1|^2 n_{ab}}{\Gamma_{ab}\Gamma_{ca}\Gamma_{cb} + \Gamma_{ab}|\Omega_1|^2 + \Gamma_{ca}|\Omega_2|^2}\Omega_2, \tag{13}$$

where $n_{\alpha\beta} = n_\alpha - n_\beta$, and $n_\alpha = \rho_{\alpha\alpha}$ is the population of level $|\alpha\rangle$, and write that for the coherence at the microwave transition as

$$\rho_{cb} = i\frac{\Gamma_{ca}n_{ab} + \Gamma_{ab}n_{ac}}{\Gamma_{ab}\Gamma_{ca}\Gamma_{cb} + \Gamma_{ab}|\Omega_1|^2 + \Gamma_{ca}|\Omega_2|^2}\Omega_1\Omega_2. \tag{14}$$

The optical coherences are related to the atomic populations in the levels as

$$\rho_{ab} = i(Z_{11}n_{ab} + Z_{12}n_{ac})\Omega_1, \tag{15}$$

$$\rho_{ca} = i(Z_{21}n_{ab} + Z_{22}n_{ac})\Omega_2, \tag{16}$$

where

$$Z_{11} = \frac{\Gamma_{ca}\Gamma_{cb} + |\Omega_1|^2}{\Gamma_{ab}\Gamma_{ca}\Gamma_{cb} + \Gamma_{ab}|\Omega_1|^2 + \Gamma_{ca}|\Omega_2|^2}, \tag{17}$$

$$Z_{12} = \frac{|\Omega_2|^2}{\Gamma_{ab}\Gamma_{ca}\Gamma_{cb} + \Gamma_{ab}|\Omega_1|^2 + \Gamma_{ca}|\Omega_2|^2}, \tag{18}$$

$$Z_{21} = \frac{|\Omega_1|^2}{\Gamma_{ab}\Gamma_{ca}\Gamma_{cb} + \Gamma_{ab}|\Omega_1|^2 + \Gamma_{ca}|\Omega_2|^2}, \tag{19}$$

$$Z_{22} = \frac{\Gamma_{ab}\Gamma_{cb} + |\Omega_2|^2}{\Gamma_{ab}\Gamma_{ca}\Gamma_{cb} + \Gamma_{ab}|\Omega_1|^2 + \Gamma_{ca}|\Omega_2|^2}. \tag{20}$$

Then the equations for the atomic populations are given by

$$\gamma_b n_a + 2|\Omega_1|^2[\mathrm{Re}(Z_{11})n_{ab} + \mathrm{Re}(Z_{12})n_{ac}] = 0,$$
$$\gamma_c n_a + 2|\Omega_2|^2[\mathrm{Re}(Z_{21})n_{ab} + \mathrm{Re}(Z_{22})n_{ac}] = 0.$$

The analytical solutions of the above equations are too complicated to be analyzed. Nevertheless, for the small detuning from the two-photon resonance, $|\Gamma_{cb}| \ll \Gamma$ and $\delta\nu \ll \Gamma$, we can find that the optical coherence is given by

$$\rho_{ab} = i\frac{n_c|\Omega_2|^2 - n_b|\Omega_1|^2 + n_a(|\Omega_1|^2 - |\Omega_2|^2)}{|\Omega_1|^2 + |\Omega_2|^2}\frac{\Omega_1}{\Gamma} - i\Gamma_{cb}\frac{(1-3n_a)|\Omega_2|^2}{(|\Omega_1|^2 + |\Omega_2|^2)^2}\Omega_1 - i\frac{(1-3n_a)\Gamma\Gamma_{cb}^2|\Omega_2|^2}{(|\Omega_1|^2 + |\Omega_2|^2)^3}\Omega_1.$$

The populations in levels $|b\rangle$ and $|c\rangle$ are given by

$$n_b = \frac{|\Omega_2|^2}{|\Omega_1|^2 + |\Omega_2|^2}, \quad n_c = \frac{|\Omega_1|^2}{|\Omega_1|^2 + |\Omega_2|^2}, \tag{21}$$

and the population in the excited state is negligible $n_a \simeq 0$. The susceptibilities for optical fields are given by

$$\chi_{ab} = \frac{\eta_{ab}\delta\nu|\Omega_2|^2}{(|\Omega_1|^2 + |\Omega_2|^2)^2} - i\frac{\eta_{ab}|\Omega_2|^2\Gamma\delta\nu^2}{(|\Omega_1|^2 + |\Omega_2|^2)^3},$$
$$\chi_{ac} = -\frac{\eta_{ac}\delta\nu|\Omega_1|^2}{(|\Omega_1|^2 + |\Omega_2|^2)^2} - i\frac{\eta_{ac}|\Omega_1|^2\Gamma\delta\nu^2}{(|\Omega_1|^2 + |\Omega_2|^2)^3},$$

where $\delta\nu = \nu_1 - \nu_2 - \omega_{cb}$. The dispersion for the optical field Ω_1 is given by

$$k_1 = \frac{\omega_{ab}}{c} + \frac{\nu_1 - \omega_{ab}}{V_{ab}}, \tag{22}$$

and that for the second optical field, by

$$k_2 = \frac{\omega_{ac}}{c} + \frac{\nu_2 - \omega_{ac}}{V_{ac}}, \tag{23}$$

where the steep dispersion is defined by

$$V_{ab} = \frac{(|\Omega_1|^2 + |\Omega_2|^2)^2}{\eta_{ab}|\Omega_2|^2}, \quad V_{ac} = \frac{(|\Omega_1|^2 + |\Omega_2|^2)^2}{\eta_{ac}|\Omega_1|^2}, \tag{24}$$

which coincide with the group velocities for the corresponding optical fields when $V_{ab}, V_{ac} \ll c$. Indeed, for the group velocities, we have $V_{g,ab} = cV_{ab}/(c + V_{ab}) \simeq V_{ab}$ and $V_{g,ac} = cV_{ac}/(c + V_{ac}) \simeq V_{ac}$.

The coherence at the microwave transition [2,3] is

$$\rho_{cb} = -\frac{\Omega_1\Omega_2}{|\Omega_1|^2 + |\Omega_2|^2}, \tag{25}$$

and the microwave field generated in the cell [see Eq. (11)] is given by

$$\Omega_3 = -i\eta_3\int_0^L dx\, e^{i(k_1 - k_2 \pm k_3)x}\rho_{cb}, \tag{26}$$

where L is the length of the cell.

III. SIMULATIONS AND OBTAINED RESULTS

A. The optical pumping scheme

In Fig. 1, we chose the linear polarizations of optical fields 1 and 2. Then the Rb level structure can be seen as a collection of the three-level atoms interacting with the optical fields, and the results obtained using the model considered in the previous section are applicable for the Rb vapor. The magnetic polarization P is generated due to the coherence between $|F = 2, m = -1\rangle$ and $|F = 1, m = -1\rangle$ levels, between $|F = 2, m = 0\rangle$ and $|F = 1, m = 0\rangle$ levels, and also between $|F = 2, m = +1\rangle$ and $|F = 1, m = +1\rangle$ levels as

$$P = \mu_- N\rho_{--} + \mu_+ N\rho_{++} + \mu_0 N\rho_{00}, \tag{27}$$

where ρ_{--}, ρ_{00} and ρ_{++} are the corresponding coherences between different pairs of magnetic sublevels for levels with $F = 2$ and $F = 1$ (see Fig. 1). The matrix elements of the z component of the magnetic dipole moment $\hat{\mu}_B = \frac{e}{2mc}(\hat{L}_z + 2\hat{S}_z)$ calculated using Eqs. (3)–(5) are

$$\mu_- = \langle F = 2, m = -1|\hat{\mu}_B|F = 1, m = -1\rangle,$$
$$\mu_0 = \langle F = 2, m = 0|\hat{\mu}_B|F = 1, m = 0\rangle, \tag{28}$$
$$\mu_+ = \langle F = 2, m = +1|\hat{\mu}_B|F = 1, m = +1\rangle.$$

Here $\mu_0 = \mu_B$, and $\mu_+ = \mu_- = \sqrt{3}/2\mu_B$ [43]. It is important to note that the moments with opposite signs of magnetic numbers have the same magnetic moments $\mu_+ = \mu_-$.

The coherences ρ_{--}, ρ_{00}, and ρ_{++} are induced via interaction with optical fields 1 and 2,

$$\rho_{--} \sim \Omega_{1-,2'-}\Omega_{2'-,2-}, \quad \rho_{++} \sim \Omega_{1+,2'+}\Omega_{2'+,2+}, \tag{29}$$

where the corresponding Rabi frequencies are $\Omega_{1\pm,2'\pm} = 1.495\, ea_0E_1/\hbar$, $\Omega_{2'\pm,2\pm} = \pm 0.863\, ea_0E_2/\hbar$, and then $\rho_{--} = -\rho_{++}$;

$$\rho_{00} \sim \Omega_{10,2'0}\Omega_{2'0,20} = 0 \tag{30}$$

because $\Omega_{2'0,20} = 0$ $(\Omega_{10,2'0} = 1.726\, ea_0E_1/\hbar)$. Thus, the magnetic polarization given by Eq. (27) is 0, and no microwave radiation can be generated. To overcome this difficulty, we

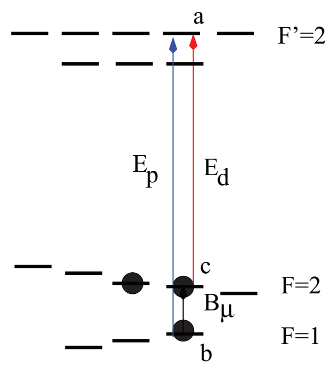

FIG. 2. (Color online) Level schemes in a weak longitudinal magnetic field that causes splitting of the ground levels ($F = 1$ and $F = 2$). The magnitude of the magnetic field is just enough to have splitting of the magnetic sublevels larger than the width of the levels due to broadening of spin transitions γ_{cb}. (We do not show the splitting of excited levels, because it is much smaller than the width of the excited states determined by the spontaneous emission rate.)

should use the optical pumping into the levels with $m = +1$ and we should have no population in levels $m = -1$.

As one can see in Fig. 2, the introduction of a weak longitudinal magnetic field along the optical beams can provide the required pumping scheme (the magnitude of the magnetic field is just enough to have splitting of magnetic sublevels larger than the width of the levels due to broadening of spin transitions γ_{cb}). Indeed, due to the the magnetic field, the two-photon resonance is going to be only for levels with $m = +1$ where the frequency difference is equal to the splitting of $|F = 2, m = -1\rangle$ and $|F = 1, m = -1\rangle$ levels, while for the other levels the optical fields are off the two-photon resonance, i.e., no coherence is generated. Moreover, the optical fields pump populations out of levels and distribute atomic populations among levels $|F = 2, m = 0\rangle$ (60% of the total population), $|F = 2, m = -1\rangle$, and $|F = 1, m = -1\rangle$ (40% of the total population) (see Fig. 2), creating the quantum coherence ρ_{cb} between the latter two levels.

The power of the generated microwave radiation can be estimated using the relation

$$|\Omega_3| \simeq \frac{\omega_{cb} N l |\wp_\mu|^2}{2c\epsilon_0\hbar}|\rho_{cb}|, \tag{31}$$

where l is the length of the cell. The estimate performed for atomic density $N \simeq 10^{13-15}$ cm^{-3} gives us a generated microwave power of as much as 30 nW/cm^2 to 3 μW/cm^2. These conditions are realistic and well suited for an experimental implementation.

We present the numerical solutions for the case of Rb vapor. The imaginary part of the susceptibility is shown in Fig. 3 as a function of the two-photon detuning $\delta\nu = \nu_1 - \nu_2 - \omega_{cb}$. The parameters are as follows: the density of Rb atoms $N = 10^{13}$ cm^{-3}, $\gamma_b \simeq \gamma_c = \gamma_r = 2 \times 10^7$ s^{-1}, the Doppler broadening [44–46] $\Delta_D = 48.5\gamma_r$, the relaxation rate for microwave transition $\gamma_{cb} = 10^4$ s^{-1}, and the length of the cell $L = 10$ cm. The Rabi frequencies Ω_1 and Ω_2 are of the order of $(0.1\text{–}10)\gamma_r$, which corresponds to a power of optical beams of about 0.1–10 mW (with a beam diameter of the order of 2–3 mm). These are the typical experimental conditions [19,39,41,42].

We can see by the manifestation of electromagnetically induced transparencyat the two-photon resonance ($\delta\nu = 0$ or $\omega_{cb} = \nu_1 - \nu_2$) that the absorption is the lowest for both fields. Correspondingly, we see a strong dispersion of the real-part susceptibility shown in Fig. 3. The important feature

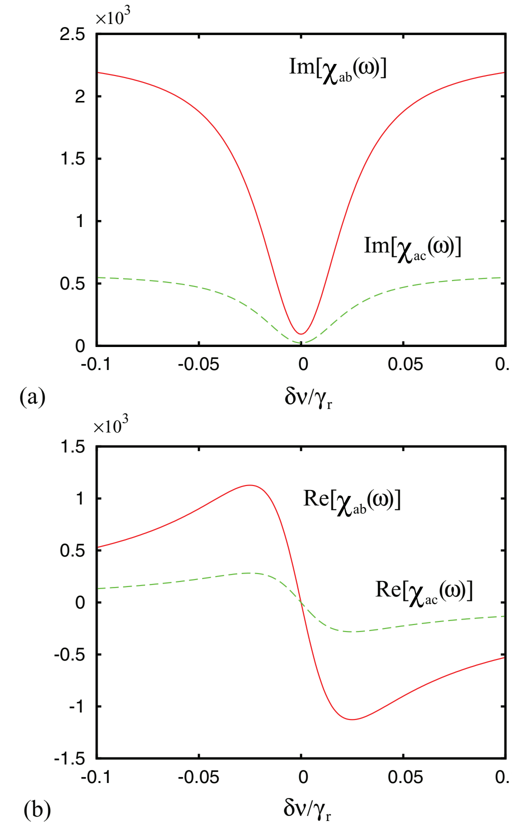

FIG. 3. (Color online) (a) Electromagnetically induced transparency for field 1 and for field 2. (b) Real part of susceptibility for field 1 and field 2.

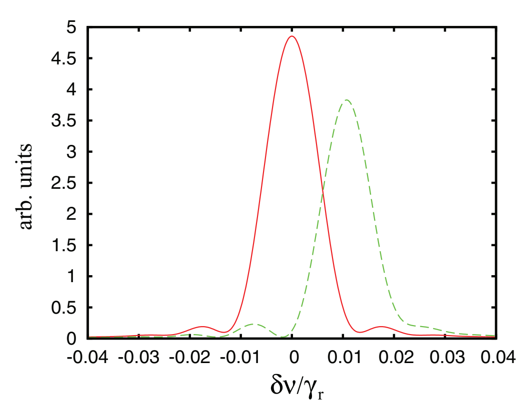

FIG. 4. (Color online) Square of the Rabi frequency $|\Omega_3|^2$ of the generated microwave field in the forward (solid line) and backward (dashed line) directions as a function of $\delta\nu$. The simulation was performed for Rabi frequencies $\Omega_1 = 1\gamma_r$ and $\Omega_2 = 3.4\gamma_r$ of the optical fields at the entrance of the cell. Other parameters are given in the text.

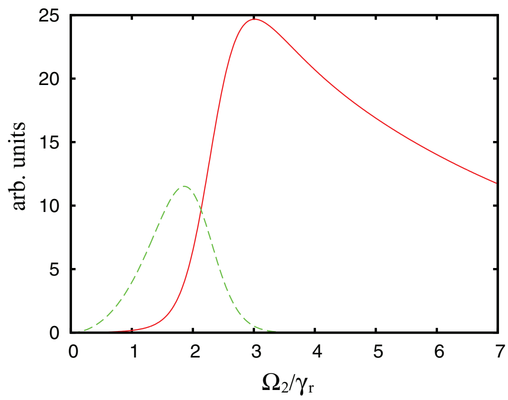

FIG. 5. (Color online) Square of the Rabi frequency $|\Omega_3|^2$ of the generated microwave field in the forward (solid line) and backward (dashed line) directions as a function of Ω_2. The simulation was performed for the Rabi frequencies $\Omega_1 = 1\gamma_r$ and two-photon detuning $\delta\nu = 0.01\gamma_r$.

is that the dispersion for each of the two fields is different, and it depends on the detuning of both fields as well as the Rabi frequency difference. Using Eqs. (22), (23), and (24), we analytically calculate the phase mismatch between the two optical fields and the propagation of the microwave field as

$$\Delta k = k_1 - k_2 - k_3 = \frac{3\lambda^2 N\gamma_r}{8\pi}\frac{|\Omega_2|^2 - |\Omega_1|^2}{(|\Omega_1|^2 + |\Omega_2|^2)^2}\delta\nu, \quad (32)$$

where $\delta\nu = \nu_1 - \nu_2 - \omega_{cb}$. We can see that in the forward direction we always have the phase matching if the fields are at the resonance $\delta\nu = \delta\nu_{1,2} = 0$. Meanwhile, in the backward direction, the phase matching can be reached by proper adjustment of the detuning or the Rabi frequencies of the optical fields so as to fulfill the condition

$$\Delta k = \frac{3\lambda^2 N\gamma_r}{8\pi}\frac{|\Omega_2|^2 - |\Omega_1|^2}{(|\Omega_1|^2 + |\Omega_2|^2)^2}\delta\nu = -2k_3. \quad (33)$$

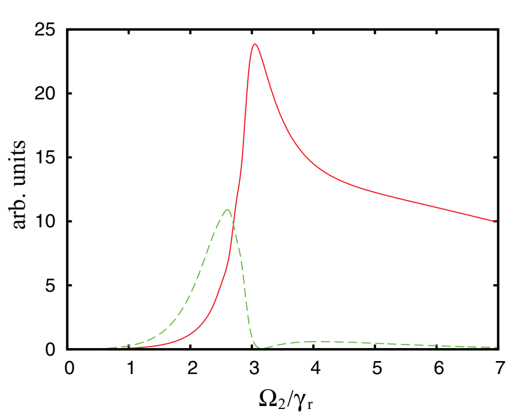

FIG. 6. (Color online) Square of the Rabi frequency $|\Omega_3|^2$ of the generated microwave field in the forward (solid line) and backward (dashed line) directions as a function of Ω_2. The simulation was performed for the Rabi frequencies $\Omega_1 = 1\gamma_r$ and two-photon detuning $\delta\nu = 0.02\gamma_r$.

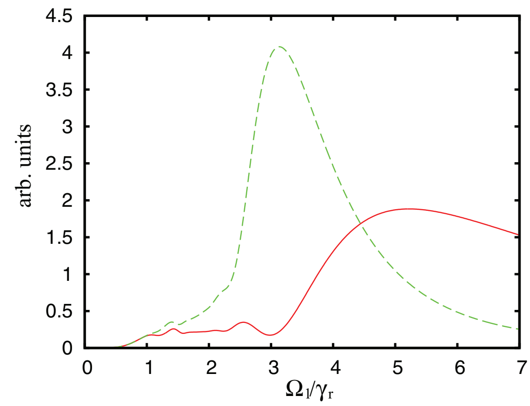

FIG. 7. (Color online) Square of the Rabi frequency $|\Omega_3|^2$ of the generated microwave field in the forward (solid line) and backward (dashed line) directions as a function of Ω_1. The simulation was performed for the Rabi frequencies $\Omega_2 = 5.4\gamma_r$ and two-photon detuning $\delta\nu = 0.01\gamma_r$.

B. Phase matching via frequency detuning

The Rabi frequency of the microwave fields generated in the cell for different parameters of the optical fields is shown in Fig. 4. For zero detuning, we see efficient generation of microwave radiation in the forward direction. And for the detuning $\delta\nu = 0.013\gamma_r$ and the parameters listed in the caption to Fig. 4, we see efficient generation of the microwave field in the backward (opposite the propagation of the optical fields) direction.

C. Phase matching by changing the driving intensities

As follows from Eq. (33), the frequency detuning is not the only parameter that can control efficient generation of microwave radiation. By changing the Rabi frequencies of optical fields even without changing the frequency detunings, we can still control the phase-matching conditions for generation of microwave radiation. In Fig. 5, the simulation for fixed two-photon detuning is shown. Upon a change in the Rabi frequency of Ω_2 we see the generation of a microwave field in the forward and backward directions. In Fig. 6, we show similar simulations with a different optical detuning $\delta\nu = 0.2\gamma_r$, and in Fig. 7 the simulations were performed by changing the Rabi frequency of Ω_1 and the two-photon detuning $\delta\nu = 0.01\gamma_r$. Again, we can state that in all demonstrated cases, we achieve efficient generation of microwave radiation in the forward and backward directions by changing the Rabi frequencies of both fields.

IV. CONCLUSION

In conclusion, we theoretically predict efficient coherent generation in the backward and forward directions while using only forward-propagating fields. This is achieved by exciting atomic coherence between hyperfine levels with properly detuned fields, in such a way that the resulting coherence creates magnetic polarization and has a spatial phase corresponding to a backward counter-propagating microwave beam.

The technique developed can be used for detection of optical as well as microwave fields [47], and it has applications to microwave modulators and optical frequency comb generation [48] that are able to control the electric and optical properties of semiconductors with microwave fields, which is important for information processing and optical communications [49]. The method also holds promise for coherent scattering and remote sensing [33], as well as for microwave-field imaging using alkali-metal atoms in a vapor cell, where the microwave field to be measured drives coherent oscillations of atomic hyperfine transitions that are detected in a spatially resolved way using a laser beam and a camera [50].

ACKNOWLEDGMENTS

We thank A. Dogariu, H. Li, and V.A. Sautenkov for useful discussions and gratefully acknowledge the partial support by the CRDF, the UNT Research Initiation Grant, and the Summer Fellowship UNT program.

APPENDIX: CONSERVATION LAWS FOR PROPAGATION IN ELECTROMAGNETICALLY INDUCED TRANSPARENCY MEDIA

The set of density matrix equations for the diagonal elements is given by

$$\dot{\rho}_{aa} = -\gamma\rho_{aa} + i(\Omega_1^*\rho_{ab} - \Omega_1\rho_{ba}) + i(\rho_{ac}\Omega_2 - \rho_{ca}\Omega_2^*),$$
$$\dot{\rho}_{bb} = \gamma_b\rho_{aa} + i(\Omega_1\rho_{ba} - \Omega_1^*\rho_{ab}) + i(\rho_{bc}\Omega_3 - \rho_{cb}\Omega_3^*),$$
$$\dot{\rho}_{cc} = \gamma_c\rho_{aa} + i(\Omega_2^*\rho_{ca} - \Omega_2\rho_{ac}) + i(\rho_{cb}\Omega_3^* - \rho_{bc}\Omega_3).$$

Using the equations above together with the propagation equations (9)–(11), allows us to obtain

$$\frac{\partial}{\partial x}\left(\frac{|\Omega_1|^2}{\eta_1} + \frac{|\Omega_2|^2}{\eta_2}\right) = \gamma\rho_{aa}, \tag{A1}$$
$$\frac{\partial}{\partial x}\left(\frac{|\Omega_1|^2}{\eta_1} + \frac{|\Omega_3|^2}{\eta_3}\right) = -\gamma_b\rho_{aa}, \tag{A2}$$
$$\frac{\partial}{\partial x}\left(\frac{|\Omega_2|^2}{\eta_2} - \frac{|\Omega_3|^2}{\eta_3}\right) = -\gamma_c\rho_{aa}. \tag{A3}$$

We assume that (a) the relaxation of spin coherence is negligible and, for the current situation, (b) there is no incoherent pumping and (c) there are no frequency or wave-number detunings $\Delta\nu = \nu_1 - \nu_2 - \nu_3 = 0$ or $\Delta k = k_1 - k_2 - k_3 = 0$. Then the population in the excited state is negligible, $\rho_{aa} \simeq 0$. Taking the coupling constant$\eta_j = \nu_j N|\wp_j|^2/(2\epsilon_0 c\hbar)$ explicitly into account, we can write

$$\frac{|\Omega_1|^2}{\eta_1} \sim \frac{|E_1|^2}{\nu_1} \sim N_1, \tag{A4}$$

where N_1 is the photon flux in the optical beam. Thus, we obtain the conservation laws for the photon fluxes in the optical and microwave beams as

$$\frac{\partial}{\partial x}(N_1 + N_2) = 0, \tag{A5}$$
$$\frac{\partial}{\partial x}(N_1 + N_3) = 0, \tag{A6}$$
$$\frac{\partial}{\partial x}(N_2 - N_3) = 0. \tag{A7}$$

[1] J. Vanier and C. Audoin, *The Quantum Physics of Atomic Frequency Standards* (Adam Hilger, Bristol, UK, 1989).

[2] E. Arimondo, in *Progress in Optics*, edited by E. Wolf, Vol. XXXV (Elsevier, Amsterdam, 1996), p. 257.

[3] M. O. Scully and M. S. Zubairy, *Quantum Optics* (Cambridge University Press, Cambridge, UK, 1997).

[4] S. E. Harris, Phys. Today **50**, 36 (1997).

[5] S. E. Harris, Phys. Rev. Lett. **85**, 4032 (2000).

[6] A. B. Matsko, Yu. V. Rostovtsev, H. Z. Cummins, and M. O. Scully, Phys. Rev. Lett. **84**, 5752 (2000).

[7] A. B. Matsko, Y. V. Rostovtsev, M. Fleischhauer, and M. O. Scully, Phys. Rev. Lett. **86**, 2006 (2001).

[8] K. J. Boller, A. Imamoglu, and S. E. Harris, Phys. Rev. Lett. **66**, 2593 (1991); S. E. Harris, *ibid.* **72**, 52 (1994).

[9] O. A. Kocharovskaya and Y. I. Khanin, Zh. Eksp. Teor. Fiz. **90**, 1610 (1986) [Sov. Phys. JETP **63**, 945 (1986)]; V. A. Sautenkov, Y. V. Rostovtsev, C. Y. Ye, G. R. Welch, O. Kocharovskaya, and M. O. Scully, Phys. Rev. A **71**, 063804 (2005).

[10] S. E. Harris, G. Y. Yin, M. Jain, and A. J. Merriam, Philos. Trans. R. Soc. London, Ser. A **355**, 2291 (1997).

[11] A. J. Merriam, S. J. Sharpe, M. Shverdin, D. Manuszak, G. Y. Yin, and S. E. Harris, Phys. Rev. Lett. **84**, 5308 (2000).

[12] H. Wang, D. Goorskey, and M. Xiao, Phys. Rev. Lett. **87**, 073601 (2001).

[13] R. Coussement, Y. Rostovtsev, J. Odeurs, G. Neyens, H. Muramatsu, S. Gheysen, R. Callens, K. Vyvey, G. Kozyreff, P. Mandel, R. Shakhmuratov, and O. Kocharovskaya, Phys. Rev. Lett. **89**, 107601 (2002).

[14] B. W. Adams, C. Buth, S. M. Cavaletto, J. Evers, Z. Harman, C. H. Keitel, A. Palffy, A. Picon, R. Rohlsbergerd, Y. Rostovtsev, and K. Tamasaku, J. Mod. Opt. **60**, 2 (2013).

[15] H. Schmidt and A. Imamoglu, Opt. Lett. **21**, 1936 (1996); S. H. Asadpour and H. R. Soleimani, Coher. Opt. Phenom. **1**, 1 (2012).

[16] A. B. Matsko, O. Kocharovskaya, Y. Rostovtsev, G. R. Welch, A. S. Zibrov, and M. O. Scully, Adv. At. Mol. Opt. Phys. **46**, 191 (2001).

[17] A. V. Turukhin, V. S. Sudarshanam, and M. S. Shahriar, J. A. Musser, B. S. Ham, and P. R. Hemmer, Phys. Rev. Lett. **88**, 023602 (2001).

[18] L. V. Hau, S. E. Harris, Z. Dutton, and C. H. Behroozi, Nature (London) **397**, 594 (1999).

[19] M. M. Kash, V. A. Sautenkov, A. S. Zibrov, L. Hollberg, G. R. Welch, M. D. Lukin, Y. Rostovtsev, E. S. Fry, and M. O. Scully, Phys. Rev. Lett. **82**, 5229 (1999); D. Budker, D. F. Kimball, S. M. Rochester, and V. V. Yashchuk, *ibid.* **83**, 1767 (1999).

[20] S. Davuluri and Y. V. Rostovtsev, Phys. Rev. A **86**, 013806 (2012); Eur. Phys. Lett. **103**, 24001 (2013).

[21] C. Y. Ye, A. S. Zibrov, Yu. V. Rostovtsev, and M. O. Scully, Phys. Rev. A **65**, 043805 (2002).

[22] E. E. Mikhailov, I. Novikova, Y. V. Rostovtsev, and G. R. Welch, Phys. Rev. A **70**, 033806 (2004).
[23] V. A. Sautenkov, Y. V. Rostovtsev, H. Chen, P. Hsu, G. S. Agarwal, and M. O. Scully, Phys. Rev. Lett. **94**, 233601 (2005).
[24] H. Xiong, M. O. Scully, and M. S. Zubairy, Phys. Rev. Lett. **94**, 023601 (2005).
[25] M. O. Scully, Phys. Rev. Lett. **55**, 2802 (1985); M. O. Scully and M. S. Zubairy, Phys. Rev. A **35**, 752 (1987).
[26] W. Schleich, M. O. Scully, and H.-G. von Garssen, Phys. Rev. A **37**, 3010 (1988); W. Schleich and M. O. Scully, *ibid.* **37**, 1261 (1988).
[27] See reviews by O. Kocharovskaya, Phys. Rep. **219**, 175 (1992); M. O. Scully, *ibid.* **219**, 191 (1992); P. Mandel, Contemp. Phys. **34**, 235 (1993); O. Kocharovskaya and P. Mandel, Quantum Opt. **6**, 217 (1994); O. Kocharovskaya, Laser Phys. **5**, 284 (1995); and the recent paper by E. A. Sete, A. A. Svidzinsky, Y. V. Rostovtsev, H. Eleuch, P. K. Jha, S. Suckewer, and M. O. Scully, IEEE J. Selected Topics Quantum Electron. **18**, 541 (2012).
[28] O. Kocharovskaya, Y. V. Rostovtsev, and A. Imamoglu, Phys. Rev. A **58**, 649 (1998).
[29] P. K. Jha, Coher. Opt. Phenom. **2**, 1 (2013).
[30] Y. V. Rostovtsev, A. B. Matsko, N. Nayak, M. S. Zubairy, and M. O. Scully, Phys. Rev. A **67**, 053811 (2003).
[31] M. O. Scully, Phys. Rev. Lett. **106**, 049801 (2011); A. A. Svidzinsky, K. E. Dorfman, and M. O. Scully, Coher. Opt. Phenom. **1**, 7 (2012).
[32] M. Jain, H. Xia, G. Y. Yin, A. J. Merriam, and S. E. Harris, Phys. Rev. Lett. **77**, 4326 (1996).
[33] M. O. Scully, G. W. Kattawar, P. R. Lucht, T. Opatrny, H. Pilloff, A. Rebane, A. V. Sokolov, and M. S. Zubairy, Proc. Natl. Acad. Sci. USA **99**, 10994 (2002).
[34] Z. E. Sariyanni and Y. V. Rostovtsev, J. Mod. Opt. **51**, 2637 (2004).
[35] G. Beadie, Z. E. Sariyanni, Y. V. Rostovtsev, T. Opatrny, J. Reintjes, and M. O. Scully, Opt. Commun. **244**, 423 (2005).
[36] Y. V. Rostovtsev, Z.-E. Sariyanni, and M. O. Scully, Phys. Rev. Lett. **97**, 113001 (2006).
[37] L. Yuan, K. E. Dorfman, A. Zheltikov, and M. O. Scully, Opt. Lett. **37**, 987 (2012).
[38] E. Kuznetsova, Y. Rostovtsev, N. G. Kalugin, R. Kolesov, O. Kocharovskaya, and M. O. Scully, Phys. Rev. A **74**, 023819 (2006).
[39] J. Vanier, A. Godone, and F. Levi, Phys. Rev. A **58**, 2345 (1998).
[40] A. Godone, F. Levi, and J. Vanier, Phys. Rev. A **59**, R12 (1999).
[41] A. Godone, F. Levi, S. Micalizio, and J. Vanier, Phys. Rev. A **62**, 053402 (2000).
[42] W. Happer, Rev. Mod. Phys. **44**, 169 (1972).
[43] Parameters for Rb atoms can be found at steck.us/alkalidata.
[44] Y. Rostovtsev, I. Protsenko, H. Lee, and A. Javan, J. Mod. Opt. **49**, 2501 (2002).
[45] H. Lee, Y. Rostovtsev, C. J. Bednar, and A. Javan, Appl. Phys. B **76**, 33 (2003).
[46] A. B. Matsko, D. V. Strekalov, and L. Maleki, Opt. Express **13**, 2210 (2005).
[47] M. Takami, Jpn. J. Appl. Phys. **15**, 1063 (1976).
[48] V. R. Supradeepa and A. M. Weiner, Opt. Lett. **37**, 3066 (2012).
[49] M. Schultze, E. M. Bothschafter, A. Sommer, S. Holzner, W. Schweinberger, M. Fiess, M. Hofstetter, R. Kienberger, V. Apalkov, V. S. Yakovlev, M. I. Stockman, and F. Krausz, Nature **493**, 75 (2013).
[50] P. Bohi and Ph. Treutlein, Appl. Phys. Lett. **101**, 181107 (2012).